High spectral resolution observations of HNC3 and HCCNC in the L1544 pre-stellar core

C. Vastel, K. Kawaguchi, D. Quénard, M. Ohishi, B. Lefloch, R. Bachiller, H. S. P. Müller

Monthly Notices of the ROYAL ASTRONOMICAL SOCIETY

MNRAS **474,** L76–L80 (2018) doi:10.1093/mnrasl/slx197
Advance Access publication 2017 December 5

High spectral resolution observations of HNC_3 and HCCNC in the L1544 pre-stellar core

C. Vastel,[1]★ K. Kawaguchi,[2] D. Quénard,[3] M. Ohishi,[4] B. Lefloch,[5] R. Bachiller[6] and H. S. P. Müller[7]★

[1]*IRAP, Université de Toulouse, CNRS, UPS, CNES, Toulouse, France*
[2]*Graduate School of National Science and Technology, Okayama University, 3-1-1 Tsushima-naka, Okayama 700-8530, Japan*
[3]*School of Physics and Astronomy, Queen Mary University of London, Mile End Road, London E1 4NS, UK*
[4]*Astronomy Data Center, National Astronomical Observatory of Japan, 2-21-1 Osawa, Mitaka, Tokyo 181-8588, Japan*
[5]*Université de Grenoble Alpes, CNRS, IPAG, F-38000 Grenoble, France*
[6]*Observatorio Astronómico Nacional (OAN, IGN), Calle Alfonso XII, 3, E-28014 Madrid, Spain*
[7]*I. Physikalisches Institut, Universität zu Köln, Zülpicher Str. 77, D-50937 Köln, Germany*

Accepted 2017 November 27. Received 2017 November 21; in original form 2017 October 21

ABSTRACT

HCCNC and HNC_3 are less commonly found isomers of cyanoacetylene, HC_3N, a molecule that is widely found in diverse astronomical sources. We want to know if HNC_3 is present in sources other than the dark cloud TMC-1 and how its abundance is relative to that of related molecules. We used the Astrochemical Studies At IRAM unbiased spectral survey at IRAM 30 m towards the prototypical pre-stellar core L1544 to search for HNC_3 and HCCNC which are by-product of the HC_3NH^+ recombination, previously detected in this source. We performed a combined analysis of published HNC_3 microwave rest frequencies with thus far unpublished millimetre data because of issues with available rest frequency predictions. We determined new spectroscopic parameters for HNC_3, produced new predictions and detected it towards L1544. We used a gas–grain chemical modelling to predict the abundances of N-species and compare with the observations. The modelled abundances are consistent with the observations, considering a late stage of the evolution of the pre-stellar core. However, the calculated abundance of HNC_3 was found 5–10 times higher than the observed one. The HC_3N, HNC_3, and HCCNC versus HC_3NH^+ ratios are compared in the TMC-1 dark cloud and the L1544 pre-stellar core.

Key words: astrochemistry – line: identification – ISM: abundances – ISM: individual objects: L1544 – ISM: molecules.

1 INTRODUCTION

Given their powerful diagnostic ability, several unbiased spectral surveys have been obtained in the past few years in the millimetre and submillimetre bands accessible from the ground obtained in the direction of star-forming regions (e.g. Herbst 2009). By far the most targeted sources are hot cores, the regions of high-mass protostars formation, where the dust temperature exceeds the sublimation temperature of the water–ice grain mantles, ∼100 K. So far, unbiased spectral surveys of low-mass solar type objects on a wide frequency range have been carried out in IRAS 16293−2422 (Blake et al. 1994; Caux et al. 2011; Jørgensen et al. 2016). The increased capabilities of the IRAM 30 m telescope make access to a new level in the investigation of molecular complexity in star-forming regions with the ASAI (Astrochemical Studies At IRAM) Large programme (see Lefloch et al., submitted to MNRAS, for a review) in the millimetre regime (project number 012-12). One of the targeted sources is the prototypical pre-stellar core, L1544, located in the Taurus molecular cloud complex (d ∼140 pc). This source is characterized by a high central density ($\geq 10^6$ cm^{-3}), a low temperature ($\leq$ 10 K), a high CO depletion, and a large degree of molecular deuteration (Crapsi et al. 2005; Vastel et al. 2006; Spezzano et al. 2013). The study of the many tracers detected in this source led to the reconstruction of its physical and dynamical structure (Keto, Rawlings & Caselli 2014). This core is also famous for being the first pre-stellar core where water has been detected (Caselli et al. 2012) and its line profile, characteristic of gravitational contraction, is confirming that L1544 is on the verge of the collapse. The ASAI high spectral resolution and high sensitivity (average rms of ∼4 mK in a 50 kHz frequency bin) led

★ E-mail: charlotte.vastel@irap.omp.eu (CV); hspm@ph1.uni-koeln.de (HSPM)

to many discoveries. For example, we have been able to obtain a full census of oxygen-bearing iCOMs (interstellar complex organic molecules), and it was found that a non-thermal desorption mechanism is possibly responsible for the observed emission of methanol and COMs from the same external layer (Vastel et al. 2014). The detection of the cyanomethyl radical (CH_2CN) for the first time in a pre-stellar core was reported by Vastel et al. (2015b), who were able to identify resolved hyperfine transitions of the *ortho* and *para* forms from the calculated frequencies. Finally, protonated cyanides, such as $HCNH^+$ and HC_3NH^+, have also been detected for the first time in a pre-stellar core (Quénard et al. 2017). The high spectral resolution of the observations allows to resolve the hyperfine structure of $HCNH^+$. The study of some nitrogen species linked to their production (HCN, HNC, HC_3N) coupled with a gas–grain chemical modelling shows that the emission of these ions originates in the external layer where non-thermal desorption of other species was previously observed.

In this study, we report on the detection of the HNC_3 species for the first time in a pre-stellar core using the ASAI IRAM-30 m spectral survey. We also report the detection of four transitions of HCCNC, one of them being already detected in the same source by Jiménez-Serra et al. (2016). The first astronomical detections of HCCNC and HNC_3 were reported by Kawaguchi et al. (1992a) and Kawaguchi et al. (1992b), respectively, towards a cold, dark molecular cloud, TMC-1. These molecules are linked to the chemistry of HC_3NH^+, previously detected in the ASAI observations. The observed line frequencies associated with HNC_3 were slightly off ($\sim$0.2 MHz) compared to the theoretical prediction given by the JPL catalogue (Pickett et al. 1998). We present in this letter the analysis of HNC_3 published microwave frequencies with millimetre data, up to 300 GHz.

2 LABORATORY SPECTROSCOPIC CONSIDERATIONS

Rest frequency predictions for the linear isocyanoacetylene (HCCNC) molecule were taken from the JPL catalogue. The entry is based on Fourier transform microwave (FTMW) and millimetre-wave (mmW) measurements (Krüger et al. 1991; Guarnieri et al. 1992), the dipole moment was determined by Krüger, Stahl & Dreizler (1993).

Iminopropadienylidene (HNC_3) is a quasi-linear molecule, i.e. an asymmetric top rotor with a low barrier to linearity (Botschwina 2003) such that rotational levels with $K_a \geq 1$ will be difficult to be observed in the laboratory, even less so in the interstellar medium. The initial predictions for HNC_3 were also taken from the JPL catalogue. The entry was based on FTMW data (Hirahara, Ohshima & Endo 1993) and additional frequencies from the radio astronomical observations (Kawaguchi et al. 1992b). We were able to tentatively assign emission lines for this species in our L1544 ASAI spectral survey. However, the predictions deviated significantly (between about 170 and 280 kHz) from our observed lines because the data employed for the initial predictions extended only to 47 GHz. Kawaguchi et al. (1992b) mentioned millimeter wave laboratory measurements of HNC_3 and published resulting spectroscopic parameters, but not the rest frequencies with their uncertainties. In this study, we combine FTMW data (Hirahara et al. 1993) displaying ^{14}N hyperfine structure (HFS) splitting with the mmW laboratory data without HFS splitting to obtain improved spectroscopic parameters; one poorly fitting weak FTMW transition frequency was omitted. The resulting parameters are shown in Table 1. Table A1 (online supplementary material) summarized experimental lines with uncertainties and residuals between measured rest-frequency and that calculated from the final spectroscopic parameters along with predictions up to 50 GHz under consideration of HFS splitting. Table A2 presents the corresponding data without HFS splitting up to 300 GHz. A dipole moment of 5.665 D was calculated by Botschwina et al. (1992). The predictions and associated files will be available in the CDMS (Endres et al. 2016).

Table 1. Spectroscopic parameters (MHz) of iminopropadienylidene (HNC_3). Numbers in parentheses are one standard deviation in units of the least significant digits.

Parameter	Value
B	4668.33576 (39)
$D \times 10^6$	618.57 (28)
eQq	1.0875 (64)

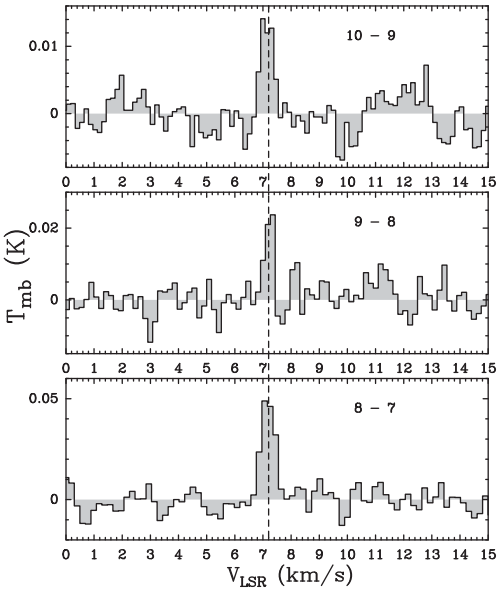

Figure 1. Three detected transitions of HNC_3 towards L1544. The vertical line shows a $V_{LSR} = 7.2\,km\,s^{-1}$.

3 OBSERVATIONS AND RESULTS

All the information concerning the observations performed at the IRAM 30 m can be found in Vastel et al. (2014) and Quénard et al. (2017). Table 2 reports the spectroscopic parameters and the properties of the detected lines, obtained by a Gaussian fitting function. For the line identification, we used the CASSIS[1] software (Vastel et al. 2015a). We present in Fig. 1 the three HNC_3 transitions and in Fig. 2 the four HCCNC transitions, detected in the ASAI spectral survey. Note that the 10–9 HCCNC transition has also been detected by Jiménez-Serra et al. (2016). Both species, as well as HC_3N already presented in Quénard et al. (2017), are produced through the HC_3NH^+ recombination reaction. This ion has previously been detected in L1544 by Quénard et al. (2017). Local thermodynamic equilibrium (LTE) analysis of HC_3NH^+ leads to a derived column density of (1–2) $\times$ 10^{11} cm^{-2}. In the case of HC_3N, a non-LTE analysis leads to the computation of a column density of (1.6–2.4) $\times$ 10^{13} cm^{-2}.

[1] http://cassis.irap.omp.eu

Table 2. Properties of the observed HNC_3 and HCCNC ($E_{up} \leq 30$ K, $A_{ul} \geq 5 \times 10^{-6}$ s^{-1}) lines. Note that the errors in the integrated intensities include the statistical uncertainties from the Gaussian fits of the lines. The rms has been computed over 20 km s^{-1}.

Transitions ($J' - J''$)	Rest frequency (MHz)	E_{up} (K)	A_{ul} (s^{-1})	FWHM (km s^{-1})	$\int T_{mb} dV$ (mK km s^{-1})	rms (mK)
			HNC_3			
8–7	74 692.1053	16.13	7.32×10^{-5}	0.57 ± 0.05	31.8 ± 5.6	4.8
9–8	84 028.2399	20.16	1.05×10^{-4}	0.34 ± 0.08	9.5 ± 4	4.5
10–9	93 364.2409	24.64	1.45×10^{-4}	0.51 ± 0.07	7.6 ± 2	2.7
			HCCNC			
8–7	79 484.1277	17.17	2.36×10^{-5}	0.41 ± 0.01	73.4 ± 2.3	4.3
9–8	89 419.2601	21.46	3.34×10^{-5}	0.37 ± 0.04	44.0 ± 9.1	2.7
10–9	99 354.2570	26.23	4.62×10^{-5}	0.44 ± 0.03	29.2 ± 4.1	2.5
11–10	109 289.1036	31.47	6.19×10^{-5}	0.45 ± 0.07	11.7 ± 3.5	3.8

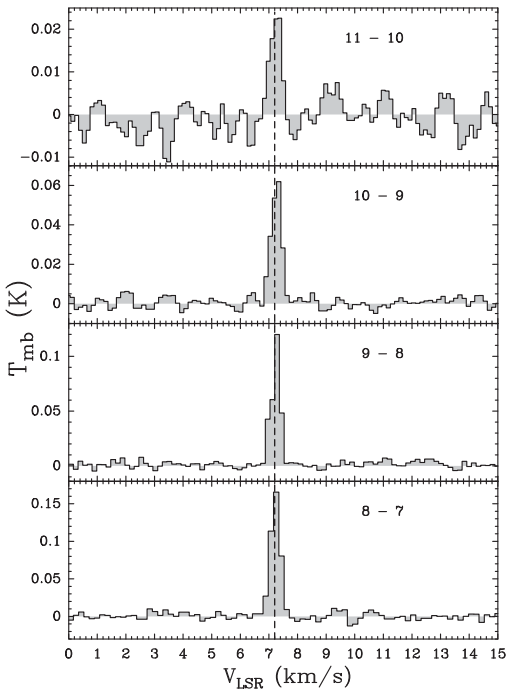

Figure 2. Four detected transitions of HCCNC towards L1544. The vertical line shows a $V_{LSR} = 7.2$ km s^{-1}.

The vertical dashed line in Fig. 2 represents the velocity in the Local Standard of Rest (V_{LSR}) of 7.2 km s^{-1} for the HCCNC species showing a good match (within 0.1 km s^{-1}) between the observed frequencies and the calculated frequencies quoted by the JPL archive data base (Pickett et al. 1998). However, the HNC_3 fitted frequencies from the JPL data base cannot be reproduced with the L1544 V_{LSR}, with an observed shift of about 1 km s^{-1}. We therefore use the frequencies as computed in Section 2 (see Table A2). In the absence of collisional coefficients for HNC_3 and HCCNC, LTE analysis has been performed using CASSIS, assuming no beam dilution. Note that LTE and non-LTE analysis for HC_3N led to similar results and we can only assume it will be the same for HNC_3 and HCCNC. The best LTE fit is obtained for a low excitation temperature of (6–8) K with column densities of (0.75–2) $\times 10^{11}$ cm^{-2} for HNC_3 and (0.85–2.2) $\times 10^{12}$ cm^{-2} for HCCNC. Jiménez-Serra et al. (2016) estimated an observed column density of (0.3–3.0) $\times 10^{12}$ cm^{-2} in a (5–10) K range using only one transition. In any case, the observed HCCNC column density is $\sim$ 10 times higher than HNC_3.

4 CHEMICAL MODELLING

Using a gas–grain chemical code (NAUTILUS, described in Ruaud, Wakelam & Hersant 2016), Quénard et al. (2017) calculated the predicted abundance using a two-step model by varying the initial gas densities of the initial phase. The resulting abundances have been compared to the observed column densities and models with an age $\geq 10^5$ yrs give a satisfactory agreement to the observations. The same modelling shows that HC_3NH^+, as well as HC_3N and HNC_3, is emitted mostly in an external layer at about 10^4 au from the centre, with a temperature of about 10 K and a density of $\sim 10^4$ cm^{-3}. When HC_3NH^+ recombines with an electron, the neutralized HC_3NH molecule has a substantial internal energy, leading to the breaking of chemical bonds. HC_3N, HNC_3, and HCCNC are all products of the HC_3NH^+ dissociative recombination (DR) reaction:

$$HC_3NH^+ + e^- \longrightarrow HC_3N + H \quad (1)$$

$$\longrightarrow HNC_3 + H \quad (2)$$

$$\longrightarrow HCCNC + H \quad (3)$$

$$\longrightarrow HCNCC + H \quad (4)$$

$$\longrightarrow HCN + C_2H \quad (5)$$

$$\longrightarrow HNC + C_2H. \quad (6)$$

Reactions (5) and (6) are not the main routes for the production of HCN and HNC, which are also products of the DR of $HCNH^+$. Also, the DR of HC_3NH^+ is not the main route for the production of HC_3N. In their theoretical analysis, Osamura et al. (1999) have chosen equal branching fractions for reactions (1) and (2) that are five times greater than those for the products in reactions (3) and (4). They also concluded that a variation from 3 to 9 (instead of 5) do not have a major effect on the calculated abundances of the metastable isomers of HC_3N. The branching ratio for the DR of DC_3ND^+ has been estimated using the heavy ion storage ring CRYRING in Stockholm, Sweden (Vigren et al. 2012) which would, in analogy with HC_3NH^+, lead to the following branching fractions: 22 per cent, 22 per cent, 4 per cent, 4 per cent, 24 per cent, and 24 per cent for reactions (1), (2), (3), (4), (5) and (6), respectively. The thermal rate coefficients for the DR of the DC_3ND^+ have been measured by Geppert et al. (2004): 1.5×10^{-6}(T/300)$^{-0.58}$ cm^3 s^{-1}. We used the KIDA data base (http://kida.obs.u-bordeaux1.fr/) and modified the HC_3NH^+ dissociative reaction rate according to

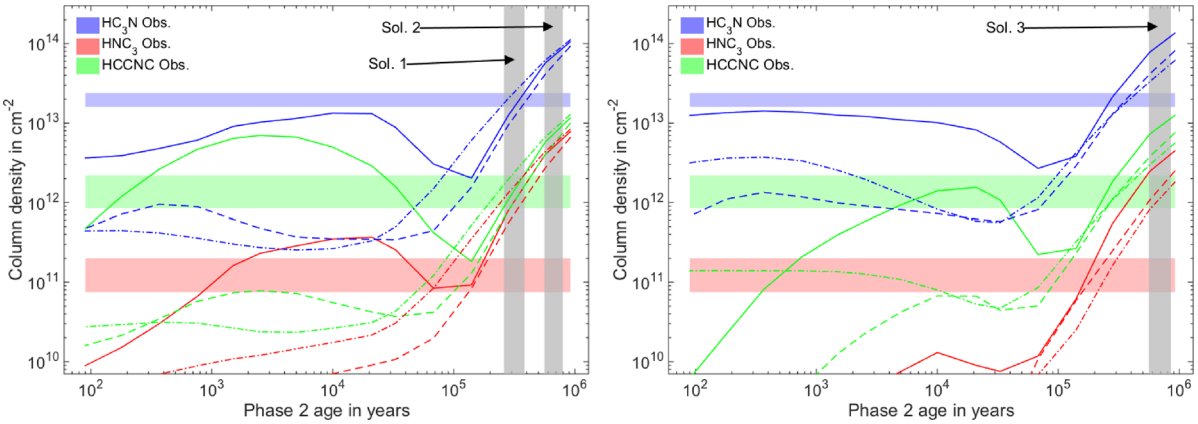

Figure 3. Column densities for HC_3N, HNC_3, and HCCNC as a function of the age of the phase 2 for different initial gas densities of the ambient cloud phase: 10^2 cm^{-3} (full line), 3×10^3 cm^{-3} (dashed line), and 2×10^4 cm^{-3} (dash–dotted line). The area of confidence of the observed column densities for these species is also shown. Grey areas show the timespan area of confidence of each model based on the observed $HCNH^+$. These areas are labelled solutions 1, 2, and 3 (Quénard et al. 2017). Left-hand panel: model EA1 of initial atomic abundances ('low-metal abundances'). Right-hand panel: model EA2 of initial atomic abundances ('high-metal abundances'). All the information on the modelling can be found in Quénard et al. (2017).

Geppert et al. (2004), using the branching ratio following Vigren et al. (2012).

Fig. B1 (online supplementary material) shows the results of the chemical modelling for the $HCNH^+$ and HC_3NH^+ ions using the modified network described above as was performed in Quénard et al. (2017). The model is divided into two phases. The first phase corresponds to the evolution of the chemistry in a diffuse or molecular cloud (hereafter ambient cloud) and depends on the assumed initial H density. The chemical composition then evolves for 10^6 yrs. The abundances from this first step are then used as initial abundances for the second step where we consider the physical structure of the L1544 pre-stellar core (Keto et al. 2014). The $HCNH^+$ and HC_3NH^+ species are emitted from the outer layer when non-thermal desorption of other species was previously observed (Vastel et al. 2014). Solutions 1, 2, and 3 (grey box in Fig. B1) represent the best comparison with the observation for the $HCNH^+$ ion (see tables 2–4 from Quénard et al. 2017). The present modelling shows that the HC_3NH^+ observations are better reproduced with the new recombination rate, compared to Quénard et al. (2017), by a factor of $\sim$ 10. We also present in Fig. 3 the comparison between the modelling and the observed column densities of HCCNC, HC_3N, and HNC_3. The HCCNC modelling is compatible with solution 1 which represents the low-metal initial abundances while HNC_3 is higher by a factor 5–10 compared to the observations. This solution has already been obtained for HC_3NH^+, HC_3N as well as other nitrogen species which have already been published by Quénard et al. (2017). We want to emphasize that, in the present network, the production of HNC_3 is dominated by the HC_3NH^+ DR while the production of HC_3N is dominated by the following reactions: C_2H_2 + CN and CH_2CCH + N. The network seems to overproduce HNC_3 compared to the observations. We present in Fig. B2 the comparison for the HNC_3 species between the chemical modelling presented in Quénard et al. (2017) and the present modified network. The destruction pathway for HNC_3 is dominated by the electron recombination for which the rate is only estimated following the experimental dissociative attachment of HNO_3 (Adams et al. 1986; Harada & Herbst 2008). Note also that the branching ratios for reactions (1)–(6) are highly uncertain, so a variation could have an impact on the chemical modelling of the aforementioned species. Note also that the HNC_3, HC_3N, and HCCNC molecules may be produced from the linear $HCCNCH^+$ ion for which we have no spectroscopic information so far.

Table 3. Comparison of the observed column densities (in cm^{-2}) between the TMC-1 dark cloud and the L1544 pre-stellar core.

	TMC-1	L1544
HC_3N	$(1.6 \pm 0.1) \times 10^{14}$	$(1.6–2.4) \times 10^{13}$
	Takano et al. (1998)	Quénard et al. (2017)
HNC_3	$(3.8 \pm 0.6) \times 10^{11}$	$(0.75–2) \times 10^{11}$
	Kawaguchi et al. (1992a)	This letter
HCCNC	$(2.9 \pm 0.2) \times 10^{12}$	$(0.85–2.2) \times 10^{12}$
	Kawaguchi et al. (1992b)	This letter
HC_3NH^+	$(1.0 \pm 0.2) \times 10^{12}$	$(1–2) \times 10^{11}$
	Kawaguchi et al. (1994)	Quénard et al. (2017)

5 COMPARISON WITH THE TMC-1 DARK CLOUD

HC_3NH^+ (two transitions), HNC_3 (three transitions), and HCCNC (three transitions) have been detected for the first time in the cold starless cloud TMC-1 [position of maximum cyanopolyyne emission: $\alpha(2000) = 04^h41^m42\overset{s}{.}47$, $\delta(2000) = +25^o41'27\overset{''}{.}1$] using the Nobeyama 45 m telescope (Kawaguchi et al. 1992a,b, 1994). Table 3 shows the comparison between the TMC-1 dark cloud and the L1544 pre-stellar core for the observations of these related species. The TMC-1 dark cloud is at an earlier stage than the L1544 pre-stellar core which is believed to be on the verge of collapse. It is important to note that, for TMC-1, the reported derived excitation temperatures for HC_3NH^+, HNC_3, and HCCNC are (6.5 ± 0.1) K, (5.0 ± 0.7) K, and (6.4 ± 0.6) K, respectively, at the lower end of the (6–8) K temperature range that we derived from the L1544 observations. The detection of the HC_3N species has been reported for the first time in TMC-1 by Suzuki et al. (1992), who reported the column density to be 1.71×10^{14} cm^{-2} using the $J = 5$–4 transition with the NRO 45 m telescope, if the excitation temperature is 6.5 K. Takano et al. (1998) then reported the analysis of the $J = 2$–1, 4–3, 5–4, and 10–9 transitions of HC_3N at the 45 m Nobeyama telescope and derived a rotational temperature of

(7.1 ± 0.1) K and column density of (1.6 ± 0.1) × 10^{14} cm^{-2}. The HC_3N/HC_3NH^+, HNC_3/HC_3NH^+, and $HCCNC/HC_3NH^+$ ratios in both sources are then similar, reflecting the cold and dense conditions in both environments: 160 ± 42, 0.4 ± 0.1, and 2.9 ± 0.8, respectively, for TMC-1, 80–240, 0.38–2, 4.25–22, respectively, for L1544.

6 CONCLUSIONS

HNC_3 has been detected for the first time in a pre-stellar core, L1544. We computed its line frequencies, necessary for the line identification and estimation of the column density. We used a gas–grain chemical modelling and compared all related nitrogen species with the observations. A comparison of the observations with the model predictions suggests that the emission from HC_3NH^+, HC_3N, HNC_3, and HCCNC originates in the outer layer where non-thermal desorption of other species was previously observed. We conclude that the modelled abundances are consistent with the observations, except for HNC_3, considering a late stage of the evolution of the pre-stellar core, compatible with previous observations.

ACKNOWLEDGEMENTS

Based on observations carried out with the IRAM 30 m Telescope. IRAM is supported by INSU/CNRS (France), MPG (Germany), and IGN (Spain). KK and MO are very grateful to S. Yamamoto and S. Saito for the opportunity to carry out laboratory spectroscopic investigations on HNC_3 at the Nagoya University. HSPM thanks Y. Endo for comments on the FTMW data of HNC_3. MO is supported by the JSPS Kakenhi grant number JP15H03646. CV would like to thank J.-C. Loison for a fruitful discussion on the reaction rates and branching fraction of the DR of the HC_3NH^+ ion. DQ acknowledges the financial support received from the STFC through an Ernest Rutherford Grant (proposal number ST/M004139).

REFERENCES

Adams N. G., Smith D., Viggiano A. A., Paulson J. F., Henchman M. J., 1986, J. Chem. Phys., 84, 6728
Blake G. A., van Dishoeck E. F., Jansen D. J., Groesbeck T. D., Mundy L. G., 1994, ApJ, 428, 680
Botschwina P., 2003, Phys. Chem. Chem. Phys., 5, 3337
Botschwina P., Horn M., Seeger S., Flügge J., 1992, Chem. Phys. Lett., 195, 427
Caselli P. et al., 2012, ApJ, 759, L37
Caux E. et al., 2011, A&A, 532, A23
Crapsi A., Caselli P., Walmsley C. M., Myers P. C., Tafalla M., Lee C. W., Bourke T. L., 2005, ApJ, 619, 379
Endres C. P., Schlemmer S., Schilke P., Stutzki J., Müller H. S. P., 2016, J. Mol. Spectrosc., 327, 95
Geppert W. D. et al., 2004, ApJ, 613, 1302
Guarnieri A., Hinze R., Krüger M., Zerbe-Foese H., Lentz D., Preugschat D., 1992, J. Mol. Spectrosc., 156, 39
Harada N., Herbst E., 2008, ApJ, 685, 272
Herbst E., van Dishoeck E., 2009, ARA&A, 47, 427
Hirahara Y., Ohshima Y., Endo Y., 1993, ApJ, 403, L83
Jiménez-Serra I. et al., 2016, ApJ, 830, L6
Jørgensen J. K. et al., 2016, A&A, 595, A117
Kawaguchi K., Ohishi M., Ishikawa S.-I., Kaifu N., 1992a, ApJ, 386, L51
Kawaguchi K. et al., 1992b, ApJ, 396, L49
Kawaguchi K., Kasai Y., Ishikawa S.-I., Ohishi M., Kaifu N., Amano T., 1994, ApJ, 420, L95
Keto E., Rawlings J., Caselli P., 2014, MNRAS, 440, 2616
Krüger M., Dreizler H., Preugschat D., Lentz D., 1991, Angew. Chem. Int. Ed., 30, 1644
Krüger M., Stahl W., Dreizler H., 1993, J. Mol. Spectrosc., 158, 298
Osamura Y., Fukuzawa K., Terzieva R., Herbst E., 1999, ApJ, 519, 697
Pickett H. M., Poynter R. L., Cohen E. A., Delitsky M. L., Pearson J. C., Müller H. S. P., 1998, J. Quant. Spectrosc. Radiat. Transfer, 60, 883
Quénard D., Vastel C., Ceccarelli C., Hily-Blant P., Lefloch B., Bachiller R., 2017, MNRAS, 470, 3194
Ruaud M., Wakelam V., Hersant F., 2016, MNRAS, 459, 3756
Spezzano S. et al., 2013, ApJ, 769, L19
Suzuki H., Yamamoto S., Ohishi M., Kaifu N., Ishikawa S.-I., Hirahara Y., Takano S., 1992, ApJ, 392, 551
Takano S. et al., 1998, A&A, 329, 1156
Vastel C., Caselli P., Ceccarelli C., Phillips T., Wiedner M. C., Peng R., Houde M., Dominik C., 2006, ApJ, 645, 1198
Vastel C., Ceccarelli C., Lefloch B., Bachiller R., 2014, ApJ, 795, L2
Vastel C., Bottinelli S., Caux E., Glorian J.-M., Boiziot M., 2015a, in Martins F., Boissier S., Buat V., Cambrésy L., Petit P., eds, SF2A-2015: Proceedings of the Annual meeting of the French Society of Astronomy and Astrophysics, p. 313
Vastel C., Yamamoto S., Lefloch B., Bachiller R., 2015b, A&A, 582, L3
Vigren E. et al., 2012, Planet. Space Sci., 60, 102

SUPPORTING INFORMATION

Supplementary data are available at *MNRASL* online.

appendix.pdf

Please note: Oxford University Press is not responsible for the content or functionality of any supporting materials supplied by the authors. Any queries (other than missing material) should be directed to the corresponding author for the letter.

This paper has been typeset from a TEX/LATEX file prepared by the author.